Analysis and Design of transformer less Single Switch based High Gain DC-DC Converter for Renewable Energy Applications

2023 11th National Power Electronics Conference (NPEC) | 979-8-3503-1164-8/23/$31.00 ©2023 IEEE | DOI: 10.1109/NPEC57805.2023.10384902

Dharavath Anusha,
National Institute of Technology Warangal
India
danusha94@gmail.com

Srinivasan Pradabane,
National Institute of Technology Warangal
India
spradabane@nitw.ac.in

***Abstract*—Conventional boost converters have limited gain with high duty ratios, high voltage stress on semiconductors, and high current ripples leads to increase in power loss and efficiency depreciation. This leads to restrict traditional boost converter in many industrial applications. A battery-grid connected non-isolated single switch high gain DC-DC (SSHGDC) converter is proposed in this paper to attain high voltage conversion ratio within limited duty ratio. The SSHGDC converter is proposed with single switch and limited number of passive elements compared to existing converters. As only one switch present in design of this converter it reduces current and voltage stress across MOSFET and further reduces switching losses. In addition, it reduces current ripples, power losses and it leads to restrict electromagnetic interferences. The advantages of proposed converter along with comparative analysis with existing topologies is tabulated in this paper. Operating principle and steady-state analysis along with design considerations and simulation results were presented.**

Keywords—High gain, voltage stress, current stress, electromagnetic interface, current ripples.

I. INTRODUCTION

The extreme usage of fossil fuel such as oil and petroleum products are leading to scarcity of fossil fuels and global warming. In-sight to this majority of global countries are adopting to renewable energy sources(RES) such as solar photo voltaic cells (PVs) [1], wind [2], fuel cells [3], and hydro power. But, the irregular and fluctuating behaviour of these RES's effects the output. Most of the RES's produces low range of voltages and less reliable [4]. To improve the reliability of RES's, batteries or super capacitors are used as energy storage devices (ESD). Power Electronic conversion technologies are used to interface between the low voltage ESDs to DC-link voltage [5]. Reliable and efficient high gain step-up DC-DC converters are used in several emerging applications such as battery storage, fuel cells, PV cells, LED lighting and X-ray power [6].

Galvanic isolation is provided by high-frequency transformers between input and output terminals of converter and by adjusting turns ratio, they employ extremely voltage gains in isolated dc-dc converters [7]-[10]. In many high power applications, the size and cost of transformer increases as turns ratio of winding increases and across active components high voltage spikes occur due transformer leakage inductance and it leads to more power dissipation. Non-isolated converters are suggested to overcome above limitations where isolation is not mandatory. The design of the traditional boost converter [11]-[13] is such that it is unable to handle higher output voltages or load current, resulting in increased conduction losses due to high voltage stress on components. Additionally, even with a very high duty ratio, the achievable gain is still low, leading to additional power wastage and decreased system efficiency. These limitations hinder its widespread usage in industrial applications where output voltage and efficiency requirements are extremely important.

Due to simple structure, compact in size and easy implementation, many of medium and low power applications uses non-isolated DC-DC converters. Based on output power requirement, switching frequency and applications, each and every topology of converter has its own advantages and limitations. Several non-isolated DC-DC converters reported in literature [14]-[23]. As large number of passive elements and semiconductor devices it is making system complex, bulky and efficiency is decreasing as the losses are increasing across them. In [14] a switched-capacitor-inductor cell based converter is proposed with the voltage gain of 3/(1-D). Converters [15] for large voltage gains for renewable energy sources whereas with voltage gain of (3-D)/(1-D) and in [16], the converter is proposed with high voltages adopting switched capacitor cell configuration wide range gain of 2/(1-D)is proposed. As the system operation is complex and mores switching stress in above converters makes it limited to fewer applications. A high gain transformer-less triple duty mode converter is proposed in [17] with voltage gain of $(2-D_2)/(1-D_1-D_2)$. As it is having more semiconductor devices shows high transients and more switching losses. A quadratic boost converter is proposed in [18] for fuel-cell based system applications with gain of $1/(1-D)^2$. In this converter additional filter circuits are required. A single switch based quadratic buck-boost converters is proposed in [19] and [20] with voltage gain of $D/(1-D)^2$ and $D^2/(1-D)^2$. In [21] gain of (1+3D)/(1-D) is proposed with single switch and four diodes. In [22] A transformer less converter is proposed with the gain of (1+D)/(1-D).

In this paper, a SSHGDC converter is proposed. A generalised diagram of proposed converter is shown in Fig. 1. The proposed SSHGDC converter includes inductor-capacitor-diode combination. Continuous mode of operation, parameter design, and comparative analysis of proposed converter along with existing converters is presented in paper. Finally duty vs gain plots are presented.

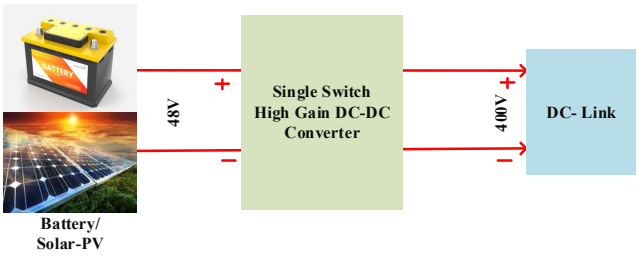

Fig. 1. Application of proposed High Gain DC-DC converter

II. Proposed SSHGDC Converter

Proposed SSHGDC converter consists of one semiconductor device (S), four diodes (D_1, D_2, D_3 and D_4), three inductors (L_1, L_2 and L_3), four capacitors (C_1, C_2, C_3 and C_4) and resistive load (R). I_{L2} and I_{L3} denotes currents across inductors L_2 and L_3 where input current (I_S) is equals to current through inductor L_1. V_{C1}, V_{C2}, V_{C3} and V_{C4} are defined as voltages across capacitors C_1, C_2, C_3 and C_4 respectively. The time period is T_S and duty ratio is denoted by D. The typical analytical waveforms during CCM operation are shown in Fig. 2. The equivalent circuit of SSHGDC converter is shown in Fig. 3. Apart from high gain the proposed converter reduces voltage and current ripples on elements.

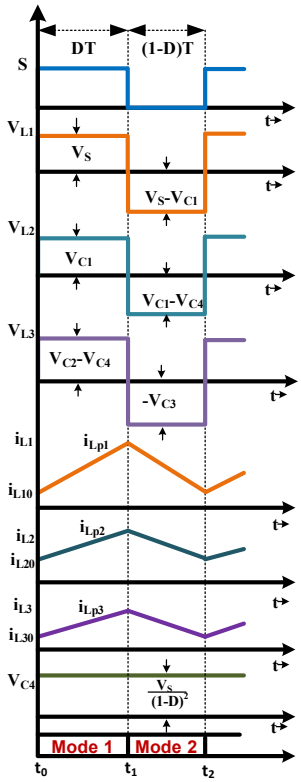

Fig. 2 Analytical waveform of SSHGDC in CCM Operation

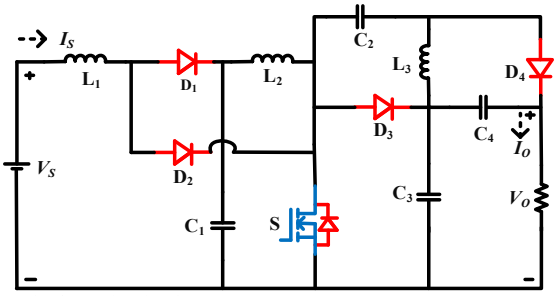

Fig. 3 Equivalent Circuit of SSHGDC

Continous Conduction Mode

Mode 1 (t_o-t_1): As shown in Fig. 3(a), switch S is turned on during time interval t_o-t_1. Inductor L_1 charges from input V_S. C_1 and V_S charges L_2, C_2 and L_3. Currents in inductor L_1, L_2 and L_3 takes positive slope as charging. Voltages across inductors L_1, L_2 and L_3 and currents through capacitors C_1, C_2, C_3, and C_4 in this mode operation are

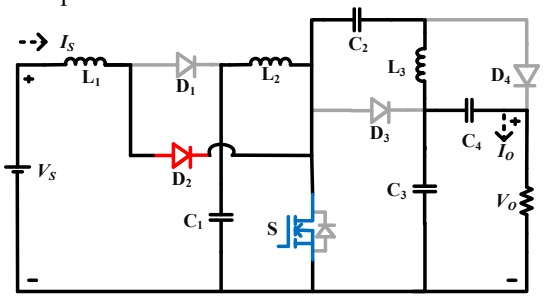

Fig. 3(a) SSHGDC in Mode-1 Operation

$$V_{L1} = V_S; V_{L2} = V_{C1}; \quad V_{L3} = V_{C2} - V_{C3}; V_o = V_{C3} + V_{C4} \tag{1}$$

$$I_{C1} = I_{L2}; I_{C2} = I_{L3}; I_{C3} = I_o; \quad I_{C4} = I_{C3} + I_{L3} = I_o + I_{L3} \tag{2}$$

Mode 2 (t_1-t_2): As shown in Fig. 3(b), switch S is turned off during time interval t_1-t_2. Inductors L_1, L_2, L_3, capacitors C_1, C_2, C_3 and C_4 discharges stored energy to load R, which increases the output voltage. L_1 charges L_2 and C_2 simultaneously. The currents in inductors L_1, L_2 and L_3 drops in negative slops while de-energized. Voltages across inductors L_1, L_2 and L_3 and currents through capacitors C_1, C_2, C_3 and C_4 in this mode operation are

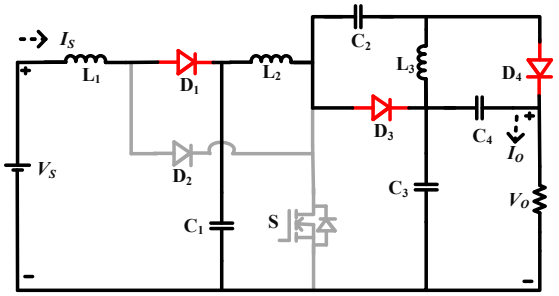

Fig. 3(b) SSHGDC in Mode-2 Operation

XXX-X-XXXX-XXXX-X/XX/$XX.00 ©20XX IEEE

$$V_{L1} = V_S - V_{C1}; V_{L2} = V_{C1} - V_{C3};$$
$$V_{L3} = -V_{C2} = -V_{C4}; V_o = V_{C3} + V_{C4} \quad (3)$$

$$I_{C1} = I_{L2} - I_{L1}; I_{C2} + I_{C4} - I_{C3} = I_{L3} - I_{L2};$$
$$I_{C2} - I_{C3} = I_{L3} - I_o \quad (4)$$

From (1) and (3), according to volt-sec balance principle voltages across capacitors are given in (5) and voltage gain equation is derived and given in (6)

$$V_{C1} = \frac{V_S}{1-D}; V_{C4} = \frac{V_{C1}}{1-D} = \frac{V_S}{(1-D)^2}; V_{C3} = DV_{C4} = \frac{DV_S}{(1-D)^2} \quad (5)$$

$$VoltageGain_{CCM} = \frac{V_o}{V_S} = \frac{1+D}{(1-D)^2} \quad (6)$$

And current gain equation is given in (7)

$$I_S = \frac{(1+D)I_o}{(1-D)^2} \quad (7)$$

III. COMPONENT DESIGN AND SELECTION

The components of the SSHGDC are designed for the V_S=48V and V_O=400V and the switching frequency (f_S) of 50 kHz. By considering the current ripple Δi_L of the inductor, the inductor currents I_{L1}, I_{L2} and I_{L3} and inductances respectively.

A. Inductor Selection

$$I_{L1} = \frac{(1+D)I_o}{(1-D)^2}; I_{L2} = \frac{(1+D)I_o}{1-D}; I_{L3} = I_o \quad (8)$$

$$L_1 = \frac{V_S D}{\Delta i_{L1} f_S}; L_2 = \frac{V_S D}{(1-D)\Delta i_{L2} f_S}; L_3 = \frac{V_S D^2}{(1-D)^2 \Delta i_{L3} f_S} \quad (9)$$

B. Capacitor Selection

Capacitors C_1, C_2, C_3 & C_4 are

$$C_1 = \frac{(1+D)DI_o}{(1-D)\Delta v_{C1} f_S}; C_2 = \frac{DI_o}{\Delta v_{C2} f_S};$$
$$C_3 = \frac{DI_o}{\Delta v_{C3} f_S}; C_4 = \frac{2DI_o}{\Delta v_{C4} f_S} \quad (10)$$

Current ripple across capacitor is defined using Δv_C.

C. Losses Caluclation

1) Inductor Losses

Losses of respective inductors are based on RMS currents are as follows

$$I_{L1} = I_{L1rms}; I_{L2} = I_{L2rms}; I_{L3} = I_{L3rms}$$
$$I_{L1rms} = I_o\left(\frac{1-D}{(1-D)^2}\right); I_{L2rms} = I_o\left(\frac{1+D}{1-D}\right); I_{L3rms} = I_o \quad (11)$$

Losses across inductors is denoted by P_{TL}

$$P_{TL} = I_{L1rms}^2 r_{L1} + I_{L2rms}^2 r_{L2} + I_{L3rms}^2 r_{L3} \quad (12)$$

Where r_{L1}, r_{L2} and r_{L3} are internal resistances of inductors L_1, L_2 and L_3 respectively

2) Capacitor Losses

Capacitor losses depends on RMS currents of respective capacitor currents.

$$i_{C1rms} = \frac{1+D}{1-D}\sqrt{\frac{D}{1-D}} I_o; i_{C2rms} = \sqrt{\frac{D}{1-D}} I_o$$
$$i_{C3rms} = \sqrt{\frac{D}{1-D}} I_o; i_{C4rms} = 2\sqrt{\frac{D}{1-D}} I_o \quad (13)$$

Turn on and turn off time of capacitor are given as

$$i_{C1on} = I_{L2}; i_{C2on} = I_{L3}; i_{C3on} = I_o; i_{C4on} = I_{L3} + i_{C3on}$$
$$i_{C1off} = I_{L2} - I_{L1}; i_{C2off} - i_{C3off} = I_{L3} - I_o \quad (14)$$
$$i_{C3off} + i_{C2off} = I_{L3}; i_{C4off} + I_{L2} + i_{C2off} = I_{L3} + I_{C3off}$$

Losses across capacitor is denoted by P_{TC}.

$$P_{TC} = i_{C1rms}^2 r_{C1} + i_{C2rms}^2 r_{C2} + i_{C3rms}^2 r_{C3} + i_{C4rms}^2 r_{C4} \quad (15)$$

Where r_{C1}, r_{C2}, r_{C3} and r_{C4} are internal resistances of respective capacitors.

3) Switching Losses

Switching losses depends on turn on and turn off time of switch. Switching loss (P_{sw}) in proposed circuit is given as

$$P_{sw} = \left(\frac{t_{on} + t_{off}}{2}\right) f_s V_s I_{sw} = \left(\frac{t_{on} + t_{off}}{2}\right) f_s \left(\frac{D}{(1-D)^2}\right) V_o I_{sw} \quad (16)$$

Conduction losses across switch is denoted by P_{swcond}

$$P_{swcond} = I_{sw}^2 * r_{sw} \quad (17)$$

Where $I_{sw} = I_{L1} + I_{L2} + I_{L3}$ and r_{sw} is internal resistance of switch

Total switching losses (P_{TSw}) are

$$P_{TSw} = P_{Sw} + P_{Swcond} \quad (18)$$

4) Diode Losses

Diode losses depends on average currents in forward direction of respective diodes.

The average currents of diodes are given as

$$i_{D1avg} = I_{L1} = I_o\left(\frac{1+D}{(1-D)^2}\right); i_{D2avg} = I_{L1} = I_o\left(\frac{1+D}{(1-D)^2}\right) \quad (19)$$
$$i_{D3avg} = I_{L2} + i_{C2off}; i_{D4avg} = I_{L3} + i_{C2off}$$

The RMS currents of diodes are given as

$$i_{D1rms} = I_o \frac{(1+D)}{(1-D)^2}\sqrt{D}; i_{D2rms} = I_o \frac{(1+D)}{(1-D)}\sqrt{\frac{1}{1-D}} \quad (20)$$
$$i_{D3rms} = I_o\sqrt{\frac{1}{1-D}}; i_{D4rms} = I_o\sqrt{\frac{1}{1-D}}$$

Forward losses (P_{DVF}) in diodes are

$$P_{DVF} = (i_{D1avg} + i_{D2avg} + i_{D3avg} + i_{D4avg}) V_{DF} \quad (21)$$

Where V_{DF} is Diode forward voltage.

Conduction losses (P_{Dcond}) in diodes are

$$P_{Dcond} = (i^2_{D1avg} + i^2_{D2avg} + i^2_{D3avg} + i^2_{D4avg}) * r_{df} \quad (22)$$

Where r_{df} is internal resistance of diode

Total Diode losses (P_{TD}) are

$$P_{TD} = P_{DVF} + P_{Dcond} \quad (23)$$

5) Total Losses

Total across of parameters are denoted as P_{Tloss}

$$P_{Tloss} = P_{TL} + P_{TC} + P_{TD} + P_{TSw}$$

$$\text{Efficiency } \eta = \frac{P_o}{P_o + P_{Tloss}}$$

Where P_O is total output power

The current and voltage stress of switch (S) and diodes (D_1, D_2, D_3 and D_4) are derived and tabulated in table-I.

Table I
Current Stress and Voltage Stress on proposed converter

	Current Stress	Voltage Stress
S	$\frac{(1+D)I_o}{(1-D)^2}$	$\frac{DV_o}{(1-D)^2}$
D_1	$\frac{(1+D)I_o}{(1-D)^2}$	$\frac{V_o}{1-D}$
D_2	$\frac{(1+D)I_o}{(1-D)^2}$	$\frac{V_o}{(1-D)^2}$
D_3	$\frac{2I_o}{1-D}$	$\frac{(1+D)V_o}{(1-D)}$
D_4	$\frac{I_o}{1-D}$	$\frac{V_o}{1-D}$

IV. Performance Comparision

A comparative study is conducted to analyze the performance of proposed SSHGDC with existing topologies. The study tabulated with component count, voltage gain, voltage stress, current stress on switch along with input and output voltages. Duty Ratio vs Voltage Gain is plotted to confirm the proposed converter gain is better during the operation of gain cycle. In Table-II comparison is tabulated and Fig. (4) represents Duty vs Gain analysis of different topologies.

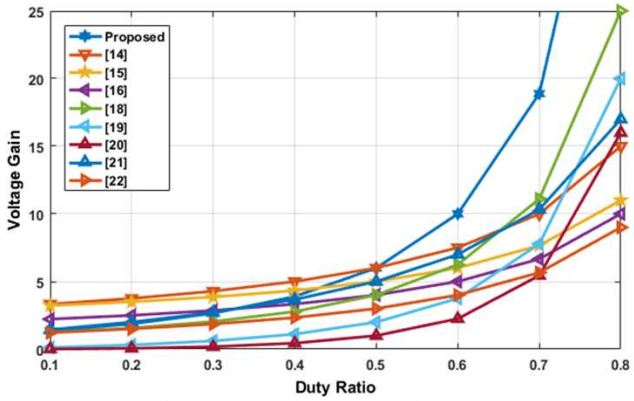

Fig. 4 Duty vs Gain plot for proposed converter and existing converters

Table- II
Comparison of Proposed Converter with existing topologies

Topology	[14]	[15]	[16]	[17]	[18]	[19]	[20]	[21]	Proposed
S	1	1	1	3	2	2	1	2	1
L	1	2	2	2	2	2	3	3	3
C	5	2	4	2	2	2	3	3	4
D	5	5	3	2	2	2	5	2	4
T	12	10	10	9	8	8	12	10	12
Gain	$\frac{3}{1-D}$	$\frac{3-D}{2-D}$	$\frac{2}{1-D}$	$\frac{2-D_2}{1-D_1-D_2}$	$\frac{1}{(1-D)^2}$	$\frac{D}{(1-D)^2}$	$\frac{D^2}{(1-D)^2}$	$\frac{1+3D}{1-D}$	$\frac{1+D}{(1-D)^2}$
Voltage stress	$\frac{V_o}{3}$	$\frac{V_o}{2}$	$\frac{V_o}{2}$	$\frac{(1-D_2)V_o}{2-D_2}$	$\frac{V_o}{(1-D)^2}$	$\frac{DV_o}{1-D}$	$\frac{V_o}{D^2}$	$\frac{V_o}{1-D}$	$\frac{DV_o}{(1-D)^2}$
Current stress	$\frac{2I_o}{1-D}$	$\frac{(1+D)I_o}{D(1-D)}$	$\frac{I_o}{1-D}$	-	$\frac{DI_o}{(1-D)^2}$	$\frac{I_o}{1-D}$	$\frac{(D^3-D^2+D)I_o}{(1-D)^2}$	$\frac{2\sqrt{D}I_o}{1+3D}$	$\frac{(1+D)I_o}{1-D}$
Input current	pulsating	pulsating	pulsating	pulsating	continuous	pulsating	continuous	pulsating	continuous
Common ground	Yes	Yes	Yes	Yes	Yes	Yes	Yes	Yes	Yes
V_s/V_o	20/200	20/100	45/380	38/400	24/200	36/215	20/200	20/260	48/400
f_s/W	200/100	100/30	100/100	200/500	50/40	50/300	40/100	50/200	50/500
Simulation Efficiency	92.40	94.89	93.5	92.3	91.7	91.4	80	94.45	96.5

S-Switch count, L- No of Inductors, C- No. of Capacitors, D- No. of Diodes, T- Total Elements

V. Simulation Results

Simulation of proposed converter is carried out in MATLAB/SIMULINK software platform. The specifications are mentioned and tabulated in Table III. Based on calculated parameters proposed converter operated on continuous conduction mode (CCM). The detailed results are presented in steady-state condition. In the SSHGDC converter, V_s= 48V, V_0= 400V with switching frequency of f_S= 50kHz at duty ratio (D)= 56.6%.

Table-III
Specification of Proposed Converter

Parameter	Specifications
Input Voltage (V_S)	48V
Output Voltage (V_O)	400V
Inductors L_1, L_2 and L_3	1mH, 1mH and 2mH
Capacitors C_1, C_2, C_3 and C_4	100µF, 100µF, 100µF and 470µF
Load (R)	320 ohm
Switch Frequency (f_s)	50kHz
Output Power (P_O)	500W
Operating Duty (D)	56.6%

For output power of 500W, given PWM pulse to switch in SSHGDC converter, the input voltage (V_S) 48V rises to output voltage (V_O) of 400V. Input current (I_S) is ~10.41A and output current I_O is ~1.25A. The simulation wave form of pulse, input and outputs (voltages and currents) along with switch voltage are shown in Fig. 5. The measured peak voltage of switch is approximately 200V. The voltage across capacitors (C_1, C_2, C_3 and C_4) are shown in Fig. 6. The measured voltages of C_1~120V, C_2~140V, C_3~ 140V and C_4~240V approximately. The diode voltages V_{D1}, V_{D2}, V_{D3}, V_{D4} are shown in Fig. 7. The measured values of V_{D1}~100V in positve phase, V_{D2}~130V, V_{D3} and V_{D4} ~230V in negative direction. Inductor voltages and currents V_{L1} V_{L2}, V_{L3}, I_{L2} and I_{L3} are shown in Fig. 8.

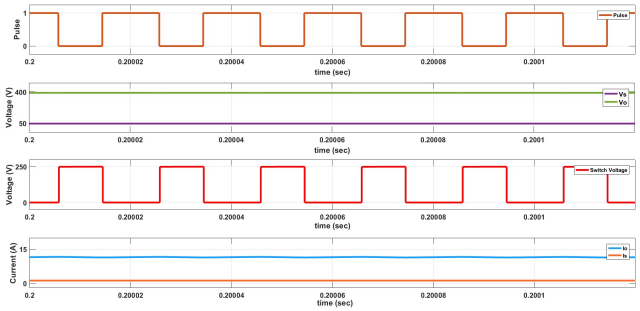

Fig. 5 Simulation Results of Pulse, input (V_S) and output voltage (V_O), switch voltage (V_{Sw}), input (I_S) and output (I_O) current from top to bottom.

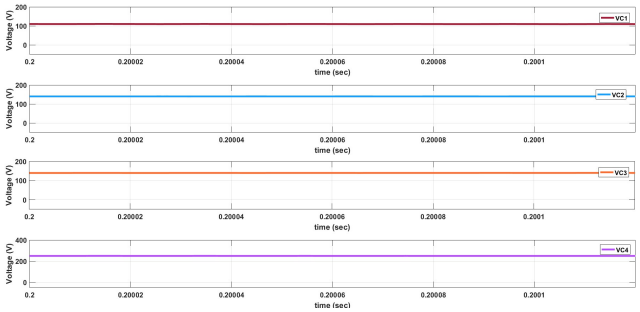

Fig. 6 Simulation Results of V_{C1}, V_{C2}, V_{C3}, V_{C4} from top to bottom.

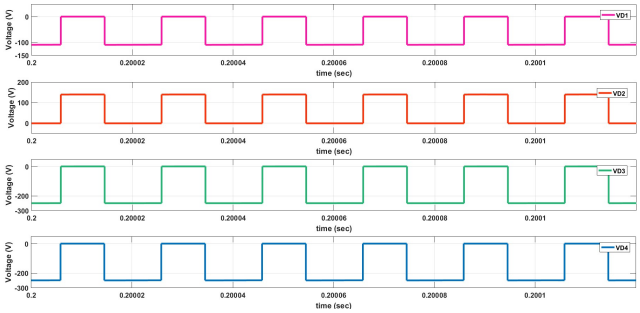

Fig. 7 Simulation Results of V_{D1}, V_{D2}, V_{D3}, V_{D4} from top to bottom.

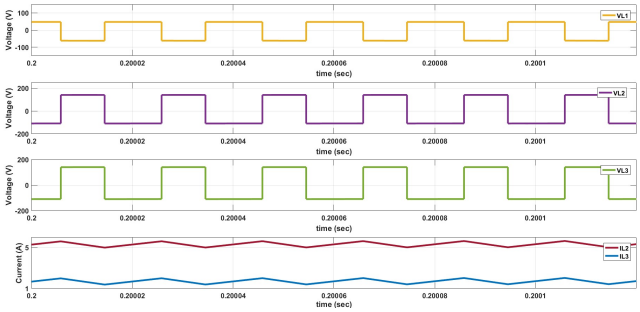

Fig. 8 Simulation Results of V_{L1}, V_{L2}, V_{L3}, I_{L2} and I_{L3} from top to bottom

VI. Conclusion

This paper presents a non-isolated single switch high gain DC-DC converter for renewable energy sources to attain high voltage conversion ratio within limited duty ratio. A new topology with a single switch and reduced number of passive elements is presented. The simulations are carried out for the proposed converter and it is found that the proposed converter could attain high gain when compared with existing converter configurations. Due to presence of only one switch, overall current and voltage stresses are reduced in the proposed converter thereby reducing the switching losses effectively as compared to existing converters. The simulation results and comparative analysis of results for existing converters and the proposed converter are presented. It can be concluded that the proposed topology is highly effective in increasing gain, reducing current stress, voltage stress, current ripples, switching losses with limited duty ratio.

REFERNCES

[1] Boico, Florent, Brad Lehman, and Khalil Shujaee. "Solar battery chargers for NiMH batteries." *IEEE Transactions on Power Electronics* 22, no. 5 (2007): 1600-1609.

[2] de Melo, Priscila Facco, Roger Gules, Eduardo Félix Ribeiro Romaneli, and Rafael Christiano Annunziato. "A modified SEPIC converter for high-power-factor rectifier and universal input voltage applications." *IEEE Transactions on Power Electronics* 25, no. 2 (2009): 310-321.

[3] Araújo, Samuel Vasconcelos, René P. Torrico-Bascopé, and Grover V. Torrico-Bascopé. "Highly efficient high step-up converter for fuel-cell power processing based on three-state commutation cell." *IEEE Transactions on Industrial Electronics* 57, no. 6 (2009): 1987-1997.

[4] Kumaravel, S. "Ultra-voltage gain bidirectional DC–DC converter with reduced switch voltage stress and improved efficiency." *IEEE Transactions on Circuits and Systems II: Express Briefs* 69, no. 11 (2022): 4468-4472.

[5] Shanthi, T., S. U. Prabha, and Kumaravel Sundaramoorthy. "Non-isolated n-stage high step-up DC-DC converter for low voltage DC source

integration." *IEEE Transactions on Energy Conversion* 36, no. 3 (2021): 1625-1634.

[6] Forouzesh, Mojtaba, Yam P. Siwakoti, Saman A. Gorji, Frede Blaabjerg, and Brad Lehman. "Step-up DC–DC converters: a comprehensive review of voltage-boosting techniques, topologies, and applications." *IEEE transactions on power electronics* 32, no. 12 (2017): 9143-9178.

[7] Ramachandran, Rakesh, and Morten Nymand. "Experimental demonstration of a 98.8% efficient isolated DC–DC GaN converter." *IEEE Transactions on Industrial Electronics* 64, no. 11 (2016): 9104-9113.

[8] Zhang, Feng, Yunxiang Xie, Yanshen Hu, Gang Chen, and Xuemei Wang. "A hybrid boost–flyback/flyback microinverter for photovoltaic applications." *IEEE Transactions on Industrial Electronics* 67, no. 1 (2019): 308-318.

[9] Spiazzi, Giorgio, and Simone Buso. "The asymmetrical half-bridge flyback converter: A reexamination." In *2020 IEEE Energy Conversion Congress and Exposition (ECCE)*, pp. 405-411. IEEE, 2020.

[10] Hu, Yihua, Rong Zeng, Wenping Cao, Jiangfeng Zhang, and Stephen J. Finney. "Design of a modular, high step-up ratio DC–DC converter for HVDC applications integrating offshore wind power." *IEEE Transactions on Industrial Electronics* 63, no. 4 (2015): 2190-2202.

[11] Arslan, Saad, Syed Asmat Ali Shah, Jae-Jin Lee, and Hyungwon Kim. "An energy efficient charging technique for switched capacitor voltage converters with low-duty ratio." *IEEE Transactions on Circuits and Systems II: Express Briefs* 65, no. 6 (2017): 779-783.

[12] Huang, Ying, Song Xiong, Siew-Chong Tan, and Shu Yuen Hui. "Nonisolated harmonics-boosted resonant DC/DC converter with high-step-up gain." *IEEE Transactions on Power Electronics* 33, no. 9 (2017): 7770-7781.

[13] Cheng, Tian, Dylan Dah-Chuan Lu, and Ling Qin. "Non-isolated single-inductor DC/DC converter with fully reconfigurable structure for renewable energy applications." *IEEE Transactions on Circuits and Systems II: Express Briefs* 65, no. 3 (2017): 351-355.

[14] Chen, Manxin, Kerui Li, Jiefeng Hu, and Adrian Ioinovici. "Generation of a family of very high DC gain power electronics circuits based on switched-capacitor-inductor cells starting from a simple graph." *IEEE Transactions on Circuits and Systems I: Regular Papers* 63, no. 12 (2016): 2381-2392.

[15] Li, Kerui, Yafei Hu, and Adrian Ioinovici. "Generation of the large DC gain step-up nonisolated converters in conjunction with renewable energy sources starting from a proposed geometric structure." *IEEE transactions on power electronics* 32, no. 7 (2016): 5323-5340.

[16] Wu, Gang, Xinbo Ruan, and Zhihong Ye. "Nonisolated high step-up DC–DC converters adopting switched-capacitor cell." *IEEE Transactions on Industrial Electronics* 62, no. 1 (2014): 383-393.

[17] Bhaskar, Mahajan Sagar, Mohammad Meraj, Atif Iqbal, Sanjeevikumar Padmanaban, Pandav Kiran Maroti, and Rashid Alammari. "High gain transformer-less double-duty-triple-mode DC/DC converter for DC microgrid." *Ieee Access* 7 (2019): 36353-36370.

[18] Wang, Faqiang. "A novel quadratic Boost converter with low current and voltage stress on power switch for fuel-cell system applications." *Renewable energy* 115 (2018): 836-845.

[19] Mayo-Maldonado, Jonathan C., Jesus E. Valdez-Resendiz, Pedro M. Garcia-Vite, Julio C. Rosas-Caro, M. del Rosario Rivera-Espinosa, and Antonio Valderrabano-Gonzalez. "Quadratic buck–boost converter with zero output voltage ripple at a selectable operating point." *IEEE Transactions on Industry Applications* 55, no. 3 (2018): 2813-2822.

[20] Zhang, Neng, Guidong Zhang, Khay Wai See, and Bo Zhang. "A single-switch quadratic buck–boost converter with continuous input port current and continuous output port current." *IEEE Transactions on Power Electronics* 33, no. 5 (2017): 4157-4166.

[21] Marcos Antonio Salvador , Telles Brunelli Lazzarin , and Roberto Francisco Coelho, "High Step-Up DC–DC Converter With Active Switched-Inductor and Passive Switched-Capacitor Networks," *IEEE Transactions on Industrial Electronics*, Vol. 65, No. 7, pp. 5644-5654,July 2018.

[22] Lung-Sheng Yang, Tsorng-Juu Liang and Jiann-Fuh Chen, "Transformerless DC–DC Converters With High Step-Up Voltage Gain", IEEE Transactions on Industrial Electronics, Vol. 56, No. 8, August 2009.